Linear conductance of quantum point contacts with deliberately broken symmetry

2006 J. Phys.: Condens. Matter 18 1715

(http://iopscience.iop.org/0953-8984/18/5/024)

INSTITUTE OF PHYSICS PUBLISHING JOURNAL OF PHYSICS: CONDENSED MATTER

J. Phys.: Condens. Matter **18** (2006) 1715–1724 doi:10.1088/0953-8984/18/5/024

Linear conductance of quantum point contacts with deliberately broken symmetry

A Shailos[1], A Ashok[1], J P Bird[2], R Akis[1], D K Ferry[1], S M Goodnick[1], M P Lilly[3], J L Reno[3] and J A Simmons[3]

[1] Nanostructures Research Group, Department of Electrical Engineering, Arizona State University, Tempe, AZ 85287-5706, USA
[2] Department of Electrical Engineering, University at Buffalo, the State University of New York, Buffalo, NY 14260-1920, USA
[3] Nanostructure and Semiconductor Physics Department, Sandia National Laboratories, PO Box 5800, Albuquerque, NM 87185-1415, USA

Received 11 October 2005, in final form 23 December 2005
Published 20 January 2006
Online at stacks.iop.org/JPhysCM/18/1715

Abstract

We investigate the linear transport properties of quantum point contacts (QPCs) whose symmetry is deliberately broken in a controlled manner. The devices that we study consist of a conventional split-gate QPC, which is modified by the inclusion of an additional perturbing gate that is used to modulate the electron density on *one* side of the device. As the voltage applied to this 'finger gate' is varied, we observe several reproducible features below the last integer plateau, as well as strong modifications of the integer-plateau staircase. Self-consistent calculations, performed for the exact device structure utilized in experiment, suggest that these features are related to the ability of the finger gate to strongly disrupt the symmetry of the QPC, reducing the electron density significantly on one side of the device. We discuss these results within the context of recent models for many-body electron transport in QPCs.

(Some figures in this article are in colour only in the electronic version)

1. Introduction

The low-temperature conductance of quantum point contacts (QPCs) is well known to be quantized in integer units of $2e^2/h$ ($\equiv G_0$) [1, 2], a result that is well explained by a model of non-interacting electron transport [3]. The same model is unable to account, however, for the presence of the additional plateau that has now been widely observed near $0.7\ G_0$ in many experiments [4–8]. The spin-related origin of this '0.7 feature' was first proposed in [4] and subsequent experiments have provided further support for this idea, suggesting the feature is connected to the spontaneous formation of a *local magnetic moment* (LMM) in the QPC. Recent work has provided evidence for the electrical readout of this LMM, by studying the characteristics of coupled QPCs [9, 10], and the notion of a spin-related phenomenon forms the

central element for many theoretical models [11–21] that attempt to account for the 0.7 feature. Among these scenarios, the LMM has been ascribed to a static (ferromagnetic) spin polarization of electrons in the QPC [16, 20, 21], and to a dynamic (Kondo-like) many-body state formed between a localized electron in the QPC and its reservoirs [17, 19]. The microscopic processes that drive the formation of the LMM are not well understood, however, and remain the subject of continued debate.

The spontaneous formation of an LMM in a QPC suggests the presence of some kind of symmetry-breaking process, which leads to the favoured occupation of electron states for one spin direction over that of the other. In many regards, this result is quite surprising, since the QPC is nominally a structure with a high degree of symmetry and no immediately obvious sources of symmetry breaking are present. In this report, we therefore explore this issue by investigating the transport properties of QPCs whose symmetry is *deliberately* broken in a controlled manner. The devices that we study consist of a conventional split-gate QPC, which is modified by the inclusion of an additional perturbing gate that is used to modulate the electron density on *one* side of the device. As the voltage applied to this 'finger gate' is varied, we observe several reproducible features below the last integer (G_0) plateau, as well as strong modifications of the integer-plateau staircase. Self-consistent calculations, performed for the exact device structure utilized in experiment, suggest that these features are related to the ability of the finger gate to strongly disrupt the symmetry of the QPC, reducing the electron density significantly on one side of the device. We discuss these results within the context of recent models for many-body electron transport in QPCs.

2. Device fabrication and basic device operation

Our devices (figure 1) were formed by depositing Ti/Au gates on top of a GaAs/AlGaAs quantum well with: a nominally undoped GaAs buffer; a GaAs/AlGaAs superlattice (300 periods); undoped $Al_{0.24}Ga_{0.76}As$ (98 nm); Si delta doping (10^{12} cm^{-2}); undoped $Al_{0.24}Ga_{0.76}As$ (95 nm); a 35 nm GaAs quantum well; undoped $Al_{0.24}Ga_{0.76}As$ (75 nm); Si delta doping (10^{12} cm^{-2}); undoped $Al_{0.24}Ga_{0.76}As$ (98 nm) and an undoped GaAs cap (10 nm). At 4.2 K, the two-dimensional electron gas (2DEG) had a density of 2.7×10^{11} cm^{-2}, a mobility of 4×10^6 cm^2 V^{-1} s^{-1}, and a mean-free path of more than 30 μm. We have studied two nominally identical devices (A and B), and a detailed investigation of device A provides the main focus of this paper. The devices were bonded into a chip carrier and mounted in the mixing chamber of a dilution refrigerator. Measurements of their conductance were made at a refrigerator temperature of 0.02 K (unless stated otherwise), using low-frequency ($\sim$11 Hz) lockin detection with constant-current excitation. The value of this current (0.5 nA) was chosen so that the voltage-drop across the devices never exceeded 30 μV, thereby ensuring that transport remained in the linear regime. After forming the QPC by applying a voltage, V_{QPC}, to the top and bottom gates in figure 1, a voltage, V_{Fing}, was then applied to one of the horizontal ('finger') gates while leaving the other floating. Due to the dimensions of the gates, and the depth of the quantum well, the main influence of varying V_{Fing} is to perturb the potential profile of the QPC (similar to the study in [22]) rather than splitting it into two distinct wires. This is confirmed by the results of self-consistent calculations of the potential profile of the QPCs (as we discuss below).

3. Experimental results

In the lower panel of figure 1, we show measurements of the conductance of device A, obtained while sweeping V_{QPC} in different directions. Although a pronounced hysteresis is

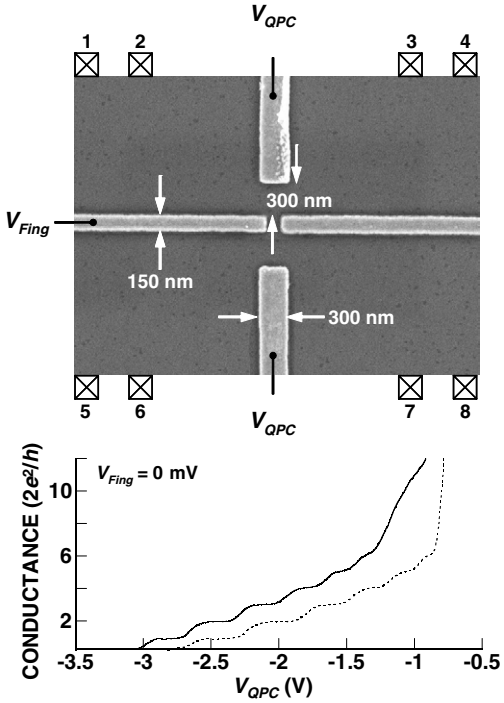

Figure 1. Top: scanning-electron microscope image, showing the gate pattern of the devices that we study. The configuration of the measurement contacts is also indicated schematically. Bottom: conductance of device A, obtained while sweeping $V_{\rm QPC}$ in different directions. Solid line: sweeping $V_{\rm QPC}$ from 0 V. Dotted line: sweeping $V_{\rm QPC}$ to 0 V.

apparent, it is clear nonetheless that the conductance shows the usual series of integer plateaus in both cases. In figure 2, we show the influence of the finger-gate on the conductance of device A, in a series of measurements performed near the last plateau. The two panels here show the results of measurements obtained by sweeping $V_{\rm QPC}$ in opposite directions. Unlike the data of figure 1, which were obtained by sweeping $V_{\rm QPC}$ over a wider range at a relatively high rate ($\Delta V_{\rm QPC} = 16$ mV s^{-1}), the data of figure 2 were obtained in very slow sweeps ($\Delta V_{\rm QPC} = 0.5$ mV s^{-1}) over a total time period of more than two weeks. These measurements reveal the presence of a variety of features in the conductance, which evolve systematically as $V_{\rm Fing}$ is varied. Noteworthy are the following. (1) A marked *hysteresis* in the conductance, which shows different features as we sweep from strong to weak (left), as opposed to weak to strong (right), QPC confinement. The hysteresis between the up and down sweeps is clearly reproducible, as evidenced by the fact that the family of curves for each sweep direction each exhibits its own, consistent, evolution. Indeed, successive sweeps of $V_{\rm QPC}$ in any specific direction, performed while keeping $V_{\rm Fing}$ fixed, were typically found to be reproducible, with no hysteresis evident. The hysteresis in figure 2 is clearly associated with a long characteristic timescale, since the time required to sweep $V_{\rm QPC}$ in either direction for any given $V_{\rm Fing}$ value was $\sim$45 min. The results of figure 1 show that the hysteresis actually persists to high conductance plateaus, ultimately collapsing as $V_{\rm QPC}$ is swept from full depletion to the range where the QPC is no longer defined. The hysteretic conductance variations indicate a systematic difference in the microscopic profile of the QPC channel, depending on whether it is formed by driving towards, or backing away from, full depletion. (2) *Missing* plateaus, at

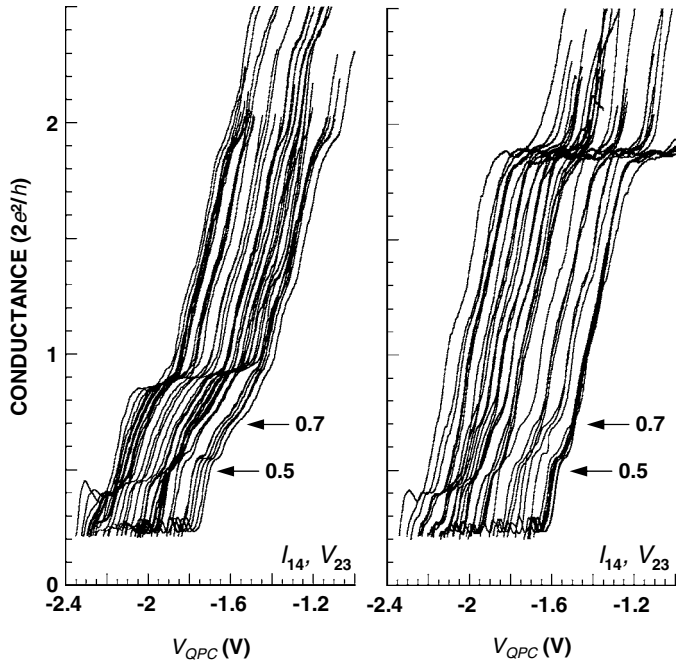

Figure 2. Conductance of device A, under different finger-gate biases. In both panels, the successive curves were obtained by incrementing the finger-gate voltage in 5 mV steps, from 0 to −185 mV. Making V_{Fing} more negative shifts the pinch-off voltage of the QPC to less negative values. In the left panel, conductance is measured while sweeping V_{QPC} towards 0 V from pinch-off, while in the right panel conductance is measured while sweeping V_{QPC} towards pinch-off, from 0 V.

2 and 1 G_0 in the left and right panels, respectively. The missing plateau in the latter case is particularly striking, since one normally expects lower plateaus to be more clearly resolved, due to an increase of the one-dimensional subband separation. In the right-hand panel of figure 2, however, the plateau at 1 G_0 is evident only as a weak inflection of the conductance in some of the curves, while the plateau at 2 G_0 is very clearly resolved for all values of V_{Fing}. (3) *Deviation* of plateaus from their quantized values, at 1 and 2 G_0 in the left and right panels, respectively. The data in figure 2 have *not* been corrected for the series resistance of the QPC reservoirs. The total resistance of these 2DEG regions is no more than 40 Ω, however, and is thus too small to account for the significant deviations of the quantized plateaus in figure 2. While the 2 G_0 plateau in the right-hand panel of figure 2 does not move significantly with gate voltage, the 1 G_0 plateau in the left-hand panel moves closer to its expected value with increasing negative finger-gate voltage. (4) The presence of *non-integer* plateau-like features, which are particularly clear below the last plateau and which evolve consistently with V_{Fing}. Prominent among these are systematically recurring plateaus near 0.7 and 0.5 G_0, with *both* features sometimes present in the *same* conductance trace. The evolution of these features appears to follow that of the 1 G_0 plateau (see the left panel of figure 2, in particular) and they are even observed in cases where this plateau is absent (figure 2, right panel). Another recurring feature occurs near 0.25 G_0.

Although device B was studied in less detail than device A, measurements of its conductance were nonetheless found to show similarities with figure 2. In figure 3, for example, we show measurements of device B at several temperatures, and for two different values of V_{Fing}. Similar to the behaviour in figure 2, hysteresis is apparent as V_{QPC} is swept as are

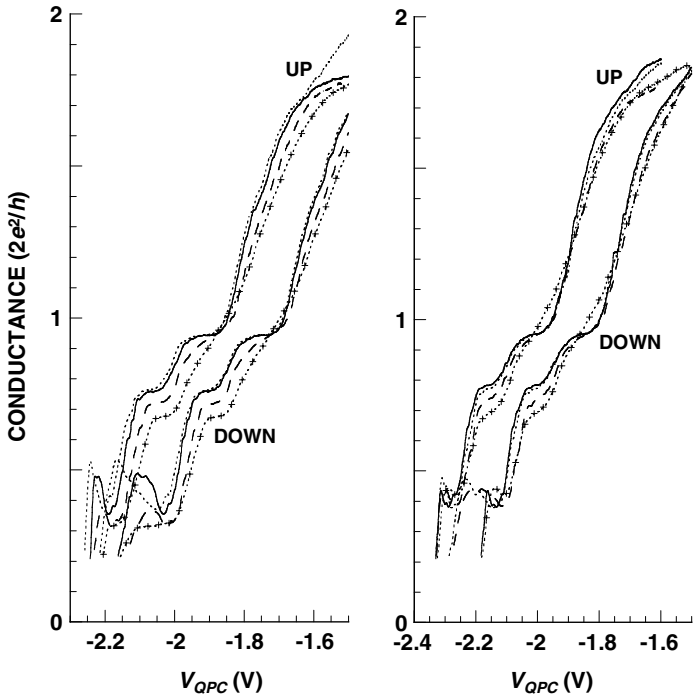

Figure 3. Temperature dependence of the conductance, measured in device B for different sweep directions (UP, $V_{\rm QPC}$ swept towards pinch-off, and DOWN, $V_{\rm QPC}$ swept away from pinch-off) with $V_{\rm Fing} = -450$ mV (left) and -425 mV (right). Solid line: 0.02 K. Dotted line: 0.4 K. Dashed line: 0.8 K. Dotted line with symbols: 1.7 K. In the two contours shown in the left-hand column, $V_{\rm QPC}$ is such that the QPC passes two modes when $V_{\rm Fing} = 0$ V. In the right-hand column, $V_{\rm QPC}$ is such that the QPC passes no modes when $V_{\rm Fing} = 0$ V.

plateau-like features near 0.7 and 0.4 G_0. At low temperatures, the 1 G_0 plateau is reduced by $\sim$7% below its normal quantized value, and this feature washes out as the temperature is increased to 1.7 K. The features near 0.7 and 0.4 G_0 remain well resolved in both panels, however, suggesting they are due to a common effect.

4. Discussion

An important new aspect of the experiments reported here is the use of the finger gate to deliberately break the symmetry of the QPC structure. For a quantitative analysis of this issue, we have used a coupled 3D Poisson/2D Schrödinger solver [23] to compute realistic potential profiles for our devices. In figure 4, we show calculated potential profiles for different combinations of $V_{\rm Fing}$ and $V_{\rm QPC}$. (The zero-energy reference in these contours is taken to be at the Fermi energy.) In the upper two contours, the finger gate is left grounded and only $V_{\rm QPC}$ is changed. The lower two contours correspond, however, to biasing with both $V_{\rm Fing}$ and $V_{\rm QPC}$. The values of $V_{\rm Fing}$ used in figure 4 are consistent with the experiment, while those for $V_{\rm QPC}$ differ by about a factor of two (see figure 2). In large part, this reflects the uncertainty in the degree of donor ionization that is assumed in the calculations for the two dopant layers. An important issue revealed by the contours in figure 4 is that activation of the finger gate does *not* split the QPC in two, but instead depletes the original electron channel formed by the QPC

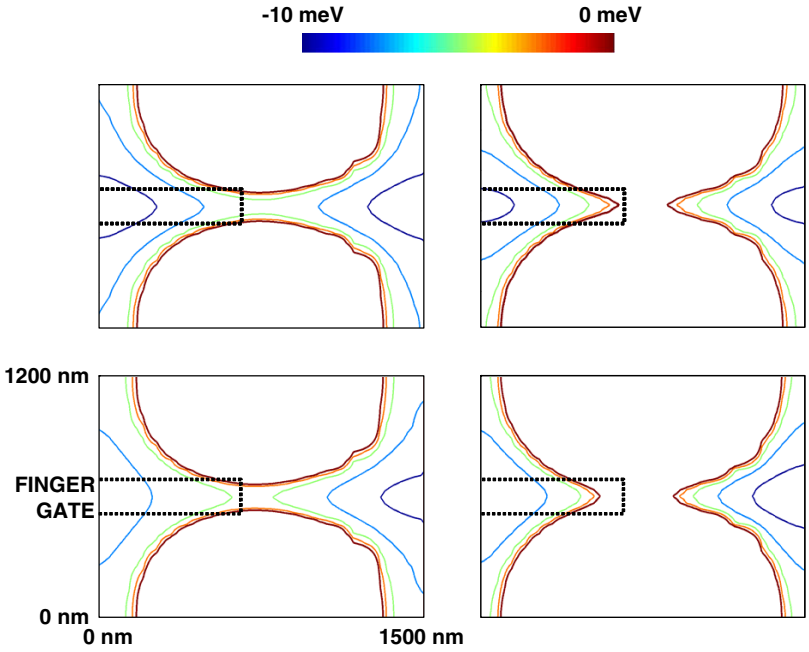

Figure 4. Calculated self-consistent potential contours for different combinations of V_{Fing} and V_{QPC}. Top left: $V_{\mathrm{QPC}} = -3.5$ V, $V_{\mathrm{Fing}} = 0$ V. Top right: $V_{\mathrm{QPC}} = -4.5$ V, $V_{\mathrm{Fing}} = 0$ V. Bottom left: $V_{\mathrm{QPC}} = -3.5$ V, $V_{\mathrm{Fing}} = -0.18$ V. Bottom right: $V_{\mathrm{QPC}} = -4.5$ V, $V_{\mathrm{Fing}} = -0.18$ V. The zero-energy reference in these contours is taken to be at the Fermi energy.

gates. Most importantly, this pinch-off arises predominantly from the depletion of carriers on one side of the QPC, as is apparent from the asymmetry of the equipotential lines in the lower two contours of figure 4. This characteristic is further revealed in figure 5, which shows the variation of the electron density as a function of V_{Fing}, at two different locations relative to the finger gate. The density changes indicated here are significant and can correspond to a variation of the local Fermi energy by an amount of the order of several meV, comparable to the typical energy spacing of the lower few subbands in split-gate QPCs [4].

The discussion above indicates that, with some important differences, the influence of the finger gate is somewhat analogous to applying a large bias voltage across the QPC. We illustrate this point schematically in figure 6, in the top panel of which we show the variation of the conduction-band edge along the direction of current flow at thermal equilibrium. In the centre panel, we show the band profile for the same QPC under conditions where a large bias is applied across its source and drain. While the carrier density in these regions is left unchanged, they are now described by different quasi-Fermi levels (or electrochemical potentials, μ_{L} and μ_{R}), which can lead to a difference in the number of QPC subbands occupied by electrons with positive and negative momentum [24]. In the lower panel, we show the situation in the experiment here, where the finger gate has been used to induce a difference in electron density between the two sides of the QPC. In this situation, the band bending may be similar to that shown in the centre panel, although an important difference in this case is that the system remains close to thermal equilibrium and the density instead differs in the source and drain.

At this point, we can only speculate on how our experimental observations are related to the deliberate symmetry breaking of the QPC by the finger gate. One of the main features of our experiments is the presence of low-index integer plateaus that are suppressed below their

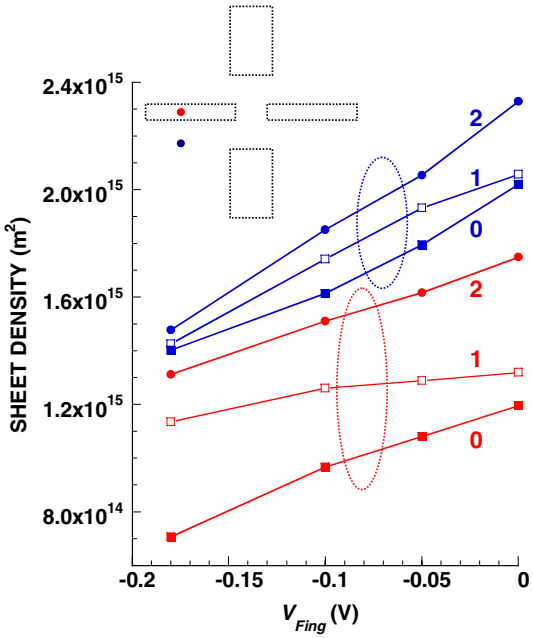

Figure 5. Calculated influence of the finger gate on the electron density near the QPC. Red and blue curves correspond to different positions with respect to the gate structure, which is indicated by dotted lines in the inset. Numbers indicate the number of modes supported by the QPC when $V_{\mathrm{Fing}} = 0$. The 2DEG density is 2.7×10^{11} cm^{-2} with all gates unbiased, in accord with the experiment.

expected quantized values (figures 2 and 3). There have been several reports of such behaviour in different semiconductor wires, which have attributed the effect to enhanced electron–electron interactions in one dimension [25, 26] and to non-adiabatic coupling to the wire reservoirs [27]. While the latter mechanism is not usually considered to be relevant for split-gate structures, it is possible that it could be important here due to the asymmetric nature of the QPC with the finger gate biased. It is also possible, however, that the reduced electron density under the finger gate could serve to enhance many-body interactions in the region near the QPC, thereby giving rise to the renormalized plateaus.

Another interesting feature of our experiments is the presence of plateau-like features near 0.7, 0.5, and 0.25 G_0 (figures 2 and 3). Prominent among these are systematically recurring plateaus near 0.7 and 0.5 G_0, with *both* features sometimes present in the *same* conductance trace. This behaviour can be seen in figure 7, which shows a histogram constructed from a large number of the traces in the left panel of figure 2. Clear peaks associated with the 1 and 2 G_0 plateaus can be identified, along with others occurring near 0.7, 0.5, and 0.25 G_0. (There even appears to be evidence for the presence of an additional feature near 1.25 G_0.) To illustrate that these multiple features can occur in the *same* conductance trace, we have highlighted the histograms for two representative data sets with different symbols. Non-integer plateaus are actually often observed in the *non-linear* conductance of QPCs, once the applied bias becomes comparable to the inter-subband spacing. Prominent among these are the so-called 'half plateaus' [24, 28], as well as features that occur near 0.25 G_0 [5, 7, 8]. It might therefore be that the multiple features that we observe below the last plateau are related to an unequal filling of forward- and backward-going momentum states that is induced by the breaking of symmetry between the source and drain.

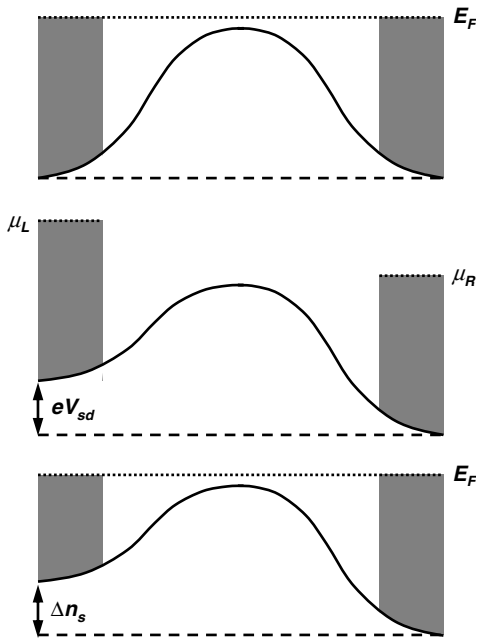

Figure 6. Schematic illustration of the conduction band edge along the direction of current flow through the QPC under different conditions. Top: thermal equilibrium. Middle: large applied source–drain bias. Bottom: induced density difference between source and drain.

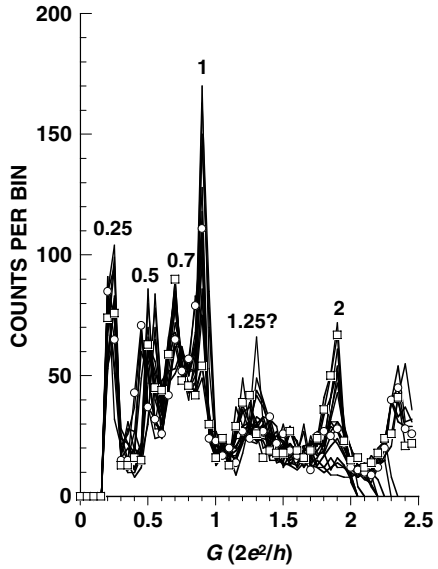

Figure 7. Conductance histogram for device A, obtained from an analysis of the conductance data in the left panel of figure 2.

An alternative interpretation of the features below the last plateau might involve *spin-polarized* transport in the QPC. Berggren and Yakimenko [16] have actually predicted the

existence of conductance anomalies at 0.7 and 0.4 G_0, due to the opening and collapse, respectively, of a spin-dependent energy gap. Other authors have predicted spin-related features near 0.75 and 0.25 G_0, due to the presence of singlet and triplet channels for transmission [11, 13]. The opening of a spin gap in the QPC could also even account for the observation of *missing* conductance plateaus, such as we find in our experiment. In the right-hand panel of figure 2, the expected plateau at 1 G_0 is absent and a stronger feature is instead observed near 0.5 G_0. To observe a plateau at 0.5 G_0, but *not* 1 G_0, its is necessary that a *large* spin gap should open, so that the two spin species show quantized transmission for *different* ranges of gate voltage. In this situation, the 0.5 G_0 plateau should denote the range where the first spin channel is completely transmitted, but the second is blocked, while the lack of a common range of quantized transmission for the two spins would result in the absence of the 1 G_0 plateau. While the appearance of a spin gap represents one possibility, it should be pointed out that other mechanisms may be responsible for the missing conductance plateaus. Büttiker has shown that, for transmission through a saddle potential, the observation of well defined conductance plateaus is strongly dependent upon the actual shape of the QPC potential [3]. In this sense, the presence of missing plateaus in our experiment may give a qualitative indication that the shape of the QPC potential evolves in a non-trivial way with gate voltage in our experiment. This may well be reasonable, given the asymmetric influence of the finger gate that is suggested by the results of figure 4.

In an earlier publication, Cronenwett *et al* provided strong evidence of a relationship of the 0.7 feature to the Kondo effect [7]. In this work, in particular, the temperature dependence of the 0.7 feature was shown to follow Kondo scaling with temperature. Figure 3 shows the temperature dependence of the quasi-plateaus that we observe near 0.7 and 0.4 G_0, in the range between 20 mK and 1.7 K. The behaviour shown here is somewhat similar to that found by Cronenwett *et al* and other workers [4, 5]; as the temperature is increased the integer quantized plateaus wash out while the quasi-plateaus at 0.7 and 0.4 G_0 are reduced in conductance and become more pronounced. This result is strongly suggestive that the multiple features that we observe are indeed related to previous observations of the 0.7 feature and do not result from some disorder-induced resonance or quantum interference.

Finally, we comment on the hysteresis that is observed in the conductance when sweeping the gates. There are many extrinsic mechanisms that could cause this behaviour, such as charging of surface states at the metal–semiconductor junction, or of impurity states within the heterostructure. While the actual mechanism responsible for the hysteresis has not been determined, in the study here it can be viewed as a useful phenomenon that allows us to evaluate the sensitivity of the QPC transport to microscopic configurational changes. In figures 2 and 3, for example, we observe the quasi-plateaus near 0.7 and 0.5 G_0, in spite of the very different variation of the background conductance. This suggests that these features are not associated with an impurity-related interference effect [29], but instead represent a more intrinsic transport signature. In addition, the experimental observation of quasi-plateaus at similar sub-G_0 values in both devices supports the idea that these features are not primarily due to disorder in the vicinity of the QPC. Further evidence for this is provided by the fact that sub-integer features with the same quantitative characteristics were found after thermal cycling of either device, suggesting that these features represent an intrinsic property of QPC transport in the few mode regime.

5. Conclusions

By making use of an additional (finger) gate, we have investigated the linear transport properties of QPCs with deliberately broken symmetry. The resulting structures exhibit a variety of

interesting effects, including both missing and renormalized integer plateaus, and multiple plateau-like features that occur below G_0. Similar behaviour was found in both of the devices that we studied, and these effects appear to be robust to changes in the precise microscopic form of the QPC potential. By demonstrating the sensitivity of QPC transport to the nature of the coupling to the reservoirs, our results should prove of relevance to the development of a realistic microscopic model for the origins of spontaneous LMM formation in these structures.

Acknowledgments

The authors gratefully acknowledge the support of the Office of Naval Research (N00014-98-0594), the National Science Foundation (ECS-0224163) and the Department of Energy (DE-FG03-01ER45920). Sandia is a multiprogramme laboratory operated by Sandia Corporation, a Lockheed Martin Company, for the United States Department of Energy's National Nuclear Security Administration under contract DE-AC04-94AL85000.

References

[1] Wharam D A, Thornton T J, Newbury R, Pepper M, Ahmed H, Frost J E F, Hasko D G, Peacock D C, Ritchie D A and Jones G A C 1988 *J. Phys. C: Solid State Phys.* **21** L209
[2] van Wees B J, van Houten H, Beenakker C W J, Williamson J G, Kouwenhoven L P, van der Marel D and Foxon C T 1988 *Phys. Rev. Lett.* **60** 848
[3] Büttiker M 1990 *Phys. Rev.* B **41** 7906
[4] Thomas K J, Nicholls J T, Simmons M Y, Pepper M, Mace D R and Ritchie D A 1996 *Phys. Rev. Lett.* **77** 135
[5] Kristensen A, Bruus H, Hansen A E, Jensen J B, Lindelof P E, Marckmann C J, Nygård J, Sørensen C B, Beuscher F, Forchel A and Michel M 2000 *Phys. Rev.* B **62** 10950
[6] Reilly D J, Facer G R, Dzurak A S, Kane B E, Stiles P J, Clark R G, Hamilton A R, Pfeiffer L N and West K W 2001 *Phys. Rev.* B **63** 121311
[7] Cronenwett S M, Lynch H J, Goldhaber-Gordon D, Kouwenhoven L P, Marcus C M, Hirose K, Wingreen N S and Umansky V 2002 *Phys. Rev. Lett.* **88** 226805
[8] Reilly D J, Buehler T M, O'Brien J L, Hamilton A R, Dzurak A S, Clark R G, Kane B E, Pfeiffer L N and West K W 2002 *Phys. Rev. Lett.* **89** 246801
[9] Morimoto T, Iwase Y, Aoki N, Sasaki T, Ochiai Y, Shailos A, Bird J P, Lilly M P, Reno J L and Simmons J A 2003 *Appl. Phys. Lett.* **82** 3952
[10] Puller V I, Mourokh L G, Shailos A and Bird J P 2004 *Phys. Rev. Lett.* **92** 96802
[11] Flambaum V V and Kuchiev M Yu 2000 *Phys. Rev.* B **61** R7869
[12] Spivak B and Zhou F 2000 *Phys. Rev.* B **61** 16730
[13] Rejec T, Ramšak A and Jefferson J H 2000 *Phys. Rev.* B **62** 12985
[14] Sushkov O P 2001 *Phys. Rev.* B **64** 155319
[15] Bruus H, Cheianov V V and Flensberg K 2001 *Physica* E **10** 97
[16] Berggren K-F and Yakimenko I I 2002 *Phys. Rev.* B **66** 085323
[17] Meir Y, Hirose K and Wingreen N S 2002 *Phys. Rev. Lett.* **89** 196802
[18] Tokura Y and Khaetskii A 2002 *Physica* E **12** 711
[19] Hirose K, Meir Y and Wingreen N S 2003 *Phys. Rev. Lett.* **90** 026804
[20] Starikov A A, Yakimenko I I and Berggren K-F 2003 *Phys. Rev.* B **67** 235319
[21] Cornaglia P S and Balseiro C A 2004 *Europhys. Lett.* **67** 634
[22] Thomas K J, Nicholls J T, Simmons M Y, Tribe W R, Davies A G and Pepper M 1999 *Phys. Rev.* B **59** 12252
[23] Vasileska D, Wybourne M N, Goodnick S M and Gunther A D 1998 *Semicond. Sci. Technol.* **13** A37
[24] Glazman L I and Khaetskii A V 1989 *Europhys. Lett.* **9** 263
[25] Tarucha S, Honda T and Saku T 1995 *Solid State Commun.* **94** 413
[26] Yacoby A, Störmer H L, Wingreen N S, Pfeiffer L N, Baldwin K W and West K W 1996 *Phys. Rev. Lett.* **77** 4612
[27] Kaufman D, Berk Y, Dwir B, Rudra A, Palevski A and Kapon E 1999 *Phys. Rev.* B **59** R10433
[28] Patel N K, Nicholls J T, Martin-Moreno L, Pepper M, Frost J E F, Ritchie D A and Jones G A C 1991 *Phys. Rev.* B **44** 13549
[29] Weis J, Haug R J, Klitzing K v and Ploog K 1992 *Phys. Rev.* B **46** 12837